Integrated Photonic Devices and Materials

Academic and Research Staff
Professor Leslie A. Kolodziejski, Dr. Gale S. Petrich, Principal Research Scientist

Graduate Students
Mohammad Araghchini, Reginald E. Bryant, Peichun (Amy) Chi, Sheila Nabanja, Orit Shamir, Ta-Ming Shih

Visiting Scientists and Research Affiliates
Prof. Hamad A. H. Brithen, Dr. Abdulmajeed Salhi

Technical and Support Staff
Denise Stewart

Introduction

The emphasis of our research program is the design, epitaxial growth, device fabrication and characterization of a number of photonic and opto-electronic structures and devices. The epitaxial growth of the heterostructures is performed in a Veeco GEN 200 solid source, multi-wafer, dual-reactor molecular beam epitaxy (MBE) system. The Veeco MBE system is capable of the epitaxial growth of dilute nitrides and antimony-based films in addition to arsenide- and phosphide-based films.

In the following sections, the status of the various research projects will be discussed. Projects include the development and simulation of rudimentary optical logic gates, the development of optical modulators for operation at 800nm, the development of saturable Bragg reflectorS for short pulse lasers and the development of long wavelength semiconductor lasers. These projects are collaborative efforts of multiple professors at MIT and members of the MIT Lincoln Laboratory technical staff enabling the successful design, simulation, fabrication and characterization of the optical devices described below.

1. Photonic Integrated Circuits for Ultrafast Optical Logic

Sponsors
Defense Advanced Research Projects Agency: Contract Number: W911NF-07-1-0630
MIT Lincoln Laboratory Integrated Photonics Initiative

Project Staff
Ta-Ming Shih, Sheila Nabanja, Dr. Jade Wang, Dr. Gale S. Petrich, Professor Rajeev Ram, Professor Erich P. Ippen, and Professor Leslie A. Kolodziejski

Today, long-distance Internet traffic is transmitted through optical fiber cables, "3R" regenerated (reamplified, reshaped, and re-timed) by optical repeaters, and routed to the desired destination. Regeneration is performed in the electronic domain, and routing can require electronic packet header processing, both of which require expensive optical-to-electronic-to-optical (OEO) conversions. OEO conversions can be alleviated by all-optical information processing. The aim of this project is to create a modular, monolithically-integrated, all-optical unit cell capable of performing a complete set of Boolean operations at speeds of over 100 Gb/s. All-optical logic operations, wavelength conversion, and other advanced optical switching schemes will be implemented using a balanced Mach-Zehnder interferometer (MZI) with a bulk InGaAsP-based semiconductor optical amplifier (SOA) in each of the interferometer's arms.

Two generations of integrated all-optical logic chips, that operate at the telecommunications wavelength of 1.55 μm, have been modeled, designed, fabricated, and are being tested. The SOAs are vertically integrated with the passive waveguides using the asymmetric twin waveguide technique. The total fabrication process consists of three contact photolithography steps and associated etch and deposition steps. Semiconductor etching is performed with an inductively-coupled plasma reactive ion etcher. The metal contacts are deposited using gold plating, after which the samples are thinned and cleaved into 2 mm by 3 mm chips. The passive waveguide losses were measured to be 0.9 cm^{-1}. Coupling losses are estimated to be approximately 7 dB per facet, due to the asymmetric shape of the waveguide mode. Lasing has been observed for non-antireflective-coated SOAs that are coupled to the passive waveguides, with the lasing threshold close to 200 mA as shown in Figure 1. Antireflective coatings were deposited onto the facets to allow for single-pass functionality measurements of the logic gates. Currently, the switching behavior is being measured. Figure 2 shows a static bias scan that is performed by measuring the transmitted power of the 1550nm light after it travels through the MZI for different combinations of SOA bias currents. The static bias scan is used to determine the bias point of the all-optical logic gate. For example, if destructive interference is desired during the "off" state of the MZI, an operating point with strong destructive interference (blue) can be chosen. If constructive interference is desired during the "off" state of the MZI, a bias point of strong constructive interference (red) can be used. Future work will include the implementation of quantum dots within the active regions of the SOAs to further increase the optical data bit rates.

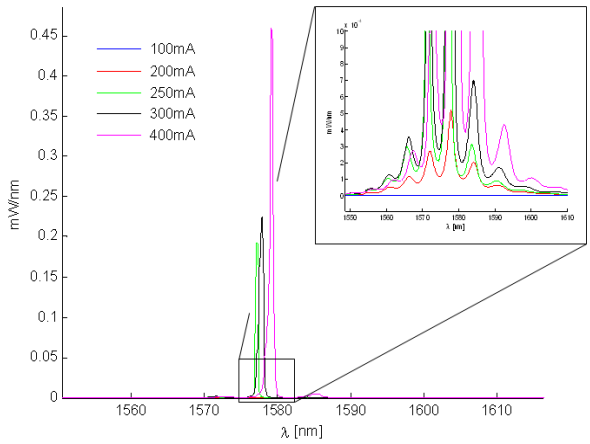

Figure 1) The lasing spectrum of a non-AR-coated 850 µm x 4 µm SOA biased at different currents.

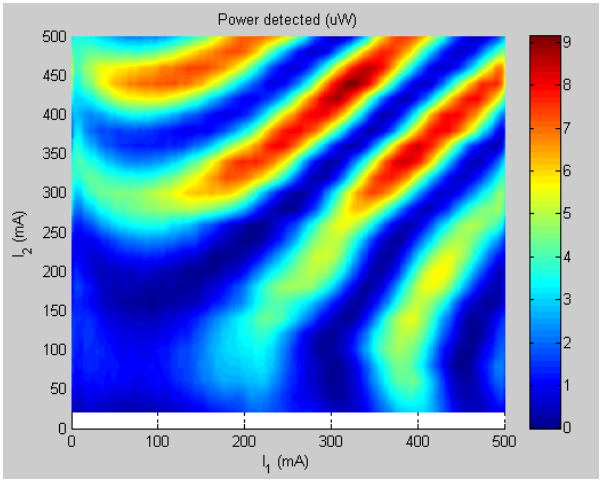

Figure 2) The static bias scan shows the interference between the two MZI arms. The x and y axes are the current that is injected into the SOA in each arm of the MZI, with the color axis being the detected output power in µW.

2. Ultra Broad Band Modulator Arrays

Sponsors
Defense Advanced Research Projects Agency: Contract Number: HR0011-05-C-0155

Project Staff
Orit Shamir, Marcus Dahlem, Dr. Gale S. Petrich, Professor Franz X. Kaertner, Professor Erich P. Ippen and Professor Leslie A. Kolodziejski

Optical signal modulation is a cornerstone of communication systems, allowing the transfer of information from the electrical domain to the optical domain. By transforming an incoming pulsed optical source into an optical frequency comb using arrayed waveguide gratings and employing both phase and amplitude modulation using Mach-Zehnder interferometers, an arbitrary optical waveform is constructed following the recombination of the frequency comb.

Electro-optic modulation of frequency combs that are centered at a wavelength of 800nm requires the use of GaAs-based materials that are transparent to light of that wavelength. A structure (shown schematically in Figure 1) consisting of alternating high- and low-index AlGaAs materials, low-index AlGaAs cladding layers, and AlAs (that can be transformed to Al_xO_y with oxidation methods) layers has been grown by molecular beam epitaxy and processed into Mach-Zehnder interferometers that consist of 2-μm-wide waveguides and active modulators. To create the largest mode possible and to minimize the coupling loss, the index contrast between the waveguiding layers and the cladding layers is minimized through the use of a dilute waveguide structure in which thin layers of high-index material are embedded in a low-index material. The resulting layered structure has an effective index slightly higher than the low-index material and is determined by the layer thicknesses as well as the refractive index of the two materials that comprise the dilute waveguide. The oxidized AlAs layers strongly confine the optical mode to the middle of the structure and are expected to allow the device to withstand higher operating voltages without concern about breakdown or carrier loss.

Fabrication of the electro-optic modulator employs a self-aligned photolithography and etching process to ensure successful optical transfer between the passive and powered waveguide regions that are defined in separate steps. The fabrication process utilizes an inductively-coupled plasma reactive ion etch (ICP-RIE) step for the definition of all waveguides to minimize the optical losses in the system. Photolithography process developments that are used in conjunction with anisotropic ICP-RIE etches, allow for consistency in the fabrication of ridge waveguides with straight sidewalls and minimal roughness. Passive measurements of fabricated structures, as seen in Figure 2, yield an optical insertion loss of 9.6db/cm using the optimized ICP-RIE processes. Successful 3dB power splitting in Y-splitters has also been observed, as shown in Figure 3.

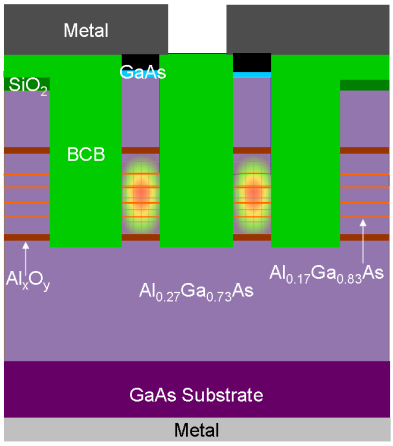

Figure 1) Cross-section illustration of a waveguide modulator structure.

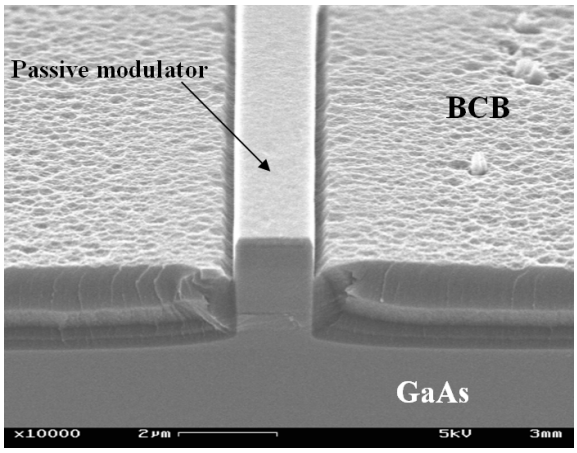

Figure 2) Facet view of the passive waveguide planarized with BCB. The waveguide leads into and out of the powered Mach-Zehnder interferometers.

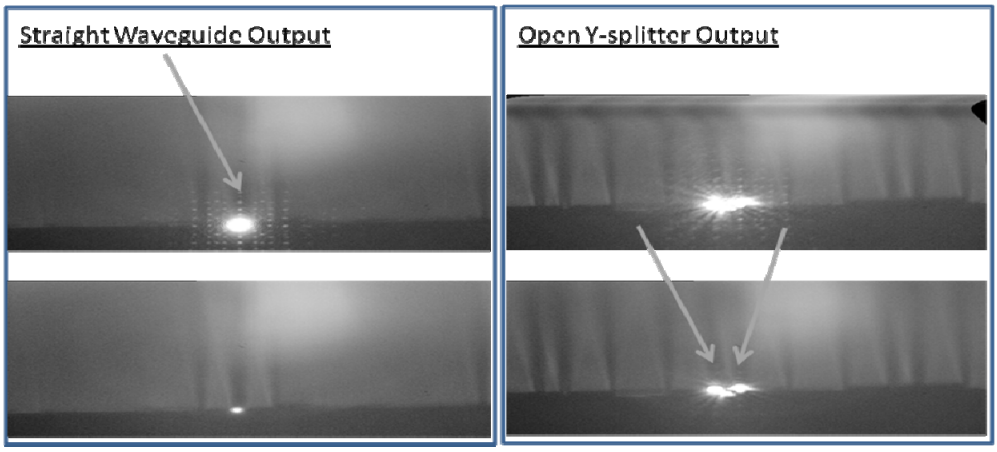

Figure 3) Facet views of successful optical transmission at the outputs of a straight waveguide (left) as well as a Y-splitter (right).

3. Mid-IR Light Sources

Sponsors:
King Abdulaziz City for Science and Technology, Award Number: 014-767-001, Thorlabs Quantum Electronics

Project Staff
Peichun (Amy) Chi, Professor Hamad A. H. Brithen, Dr. Abdulmajeed Salhi, Dr. Peter Heim, Dr. Gale S. Petrich, and Professor Leslie A. Kolodziejski

A mid-infrared (Mid-IR) semiconductor laser device is of great importance in terms of use in ultra sensitive molecular sensing applications, since several crucial toxic gas molecules (CH_4, CO_2, CO, and HCl) have their fundamental absorption lines within the spectral region spanning from 2 to 4 μm. Mid-IR laser diodes, operating at room temperature and emitting tens of milliwatts of power, can be designed in two major material systems: the antimonide-based material system and arsenide-phosphide-based material system. Sb-based devices can be designed to be nearly lattice-matched to GaSb, while the arsenide-phosphide-based devices emit around 2 μm if more than 1.5% of strain is incorporated in the quantum wells (QWs). In this work, a series of aluminum-cladded, phosphide-based laser structures with strained InGaAs quantum wells were grown and characterized (see Table 1). The laser structures were characterized by high resolution X-ray diffraction, photoluminescence (PL), and electroluminescence (EL). The light-current (L-I) and thermal resistance characteristics on ridge waveguide lasers were also measured.

Sample ID	QW composition	# QWs	Emission Wavelength
VA153	$In_{0.66}Ga_{0.34}As$	2	1.785 μm
VA154	$In_{0.66}Ga_{0.34}As$	3	1.796 μm
VA158	$In_{0.71}Ga_{0.29}As$	2	1.876 μm
VA159	$In_{0.71}Ga_{0.29}As$	3	1.907 μm
VA162	$In_{0.74}Ga_{0.26}As$	2	1.966 μm
VA163	$In_{0.75}Ga_{0.25}As$	3	2.006 μm

Table 1) Various laser structures that have been fabricated along with their quantum well composition, number of quantum wells, and lasing emission wavelength.

The laser structures were composed of strained InGaAs QWs with barriers of $In_{0.48}Ga_{0.42}Al_{0.1}As$ and that are sandwiched between $In_{0.48}Ga_{0.42}Al_{0.1}As$ waveguide layers. InP acts as the cladding layers in these separate confinement heterostructures. Figure 1 shows that the PL emission wavelength increases from 1790 nm to 1970 nm with increasing indium, or equivalently strain, in the QWs.

Figure 2 shows the continuous-wave room temperature optical spectrum and the L-I-V curve for the example laser that emitted at 1966nm. The maximum output power of this laser was 10 mW. The internal loss (α_i) and current injection efficiency (η_i) were calculated to be 44.3 cm^{-1} and 67.4%, respectively from 1.0mm and 1.5mm long devices. The laser was driven by a continuous current source and was mounted epi-side down to minimize heating effects. This 1.97 μm emitting laser is being mounted in a butterfly package with a fiber pig-tail, to allow the laser to be used in a photo-acoustic spectroscopy cell for petrochemical trace gas sensing.

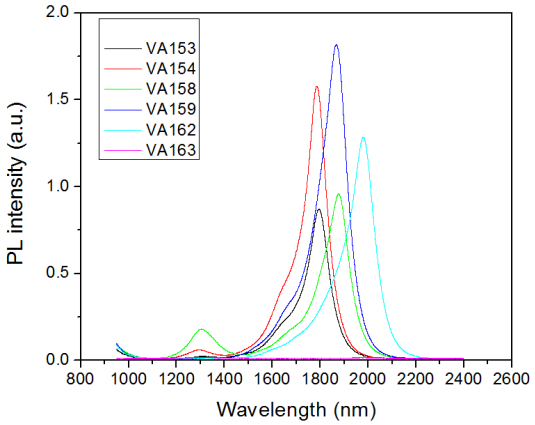

Figure 1) Compilation of PL spectra from numerous laser structures.

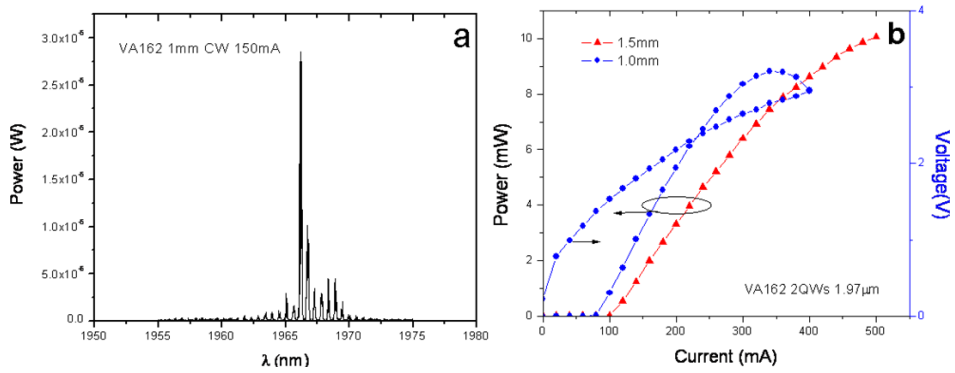

Figure 2) Laser VA162 with its a) optical power spectrum, b) continuous wave L-I-V curve at room temperature.

4. Saturable Bragg Reflectors for Ultrashort Pulse Lasers

Sponsors
Defense Advanced Research Projects Agency: Contract Number: HR0011-05-C-0155, Thorlabs Inc.

Project Staff
Sheila Nabanja, Umit Demirbas, Jonathan R. Birge, Michelle Y. Sander, Dr. Gale S. Petrich, Professor Franz X. Kaertner, Professor James G. Fujimoto, Professor Erich P. Ippen, and Professor Leslie A. Kolodziejski

Continuously pumped laser systems do not automatically generate light pulses. Barring a mechanism for mode-locking, a laser system emits at a variety of modes that are out of phase with each other, and hence the laser generates a continuous beam of light. A laser can emit short pulses of light if all the longitudinal modes within a laser cavity are locked in-phase with each other. Mode-locking can be achieved by a number of ways which are either passive or active. The prevailing method for ultra-short pulse generation is via Kerr-Lens Modelocking (KLM) which utilizes the non-linearity of the gain medium. The challenges of passive KLM mode-locking method include the difficulty causing the laser to emit pulses in a self-starting fashion and its sensitivity to vibrations.

If instead, one of the mirrors of the conventional laser cavity is replaced by a monolithically integrated saturable absorber and a highly reflective mirror, the challenges that were mentioned above with KLM can be addressed. The advantages of using a saturable absorber are that the mode-locking process is self-starting and that the pulsed mode of operation is stable from environmental fluctuations. A saturable absorber is a semiconductor that absorbs photons according to its energy band gap and initiates mode-locking by introducing an intensity-dependent loss into the laser cavity by selectively absorbing low-intensity light while transmitting light that is at a sufficiently high intensity. The highly reflective mirror is typically a distributed Bragg reflector (DBR) that is composed of materials with different indices of refraction (n) and with each layer having a thickness of $\lambda/4n$. As the index contrast between the layers increases, the high reflectivity bandwidth of the DBR increases. In order for the saturable absorber and the mirror to effectively initiate mode-locking, the sum of their parts must be capable of handling the wide bandwidth that is associated with the ultrashort pulse.

In this work, saturable Bragg reflectors (SBRs) have been grown via molecular beam epitaxy to work in lasers that operate at a center wavelength of 800nm, 850nm, 910nm and 1550nm. In most instances, the highly reflective dielectric mirror stack consists of a series of alternating layers of high index $Al_xGa_{1-x}As$ layers where $x<0.2$ and low index $Al_{0.95}Ga_{0.05}As$ layers. For SBRs with the largest reflectivity bandwidth, the dielectric mirror stack contains Al_xO_y as the low index material. In these oxide-containing SBRs, the Al_xO_y is formed by the thermal oxidation of the as-grown AlAs layers. Figure 1 shows an as-grown SBR structure prior to the thermal oxidation of AlAs and the final SBR structure with the Al_xO_y low index layers within the dielectric mirror stack. Using the Al_xO_y based SBRs (with a 6nm thick strained InGaAs quantum well as the saturable absorber) in a diode-pumped Cr^{3+}:LiSAF laser, the central wavelength of the resultant optical pulses was continuously tuned from 800 nm to 905 nm by the rotation of a specially designed birefringent plate. Within the laser's tuning range, the pulse widths varied from 70-fs to 254-fs, with an average pulse width of 139-fs. Figure 2 shows the optical spectrum of the optical pulses within the tuning range of the Cr:LiSAF laser along with the calculated reflectivity of the SBR. The oxidation process is currently being optimized to increase the usable size of the SBRs as well as to reduce the non-saturable losses, which currently limits its use within the Cr^{3+}:LiSAF laser.

Currently, we have demonstrated devices with center wavelengths ranging from 800-1550nm, we are also fabricating SBRs for lasers operating at wavelengths of 2-3μm. Narrowband (60nm) mirrors, as well as broadband (300-500nm) mirrors (with small-area oxidized mesas) have been fabricated. As a next step, we will develop broadband SBRs with larger area (>500microns) and also extend the oxidized mirror approach to the whole operating wavelength (800-3000nm) regime.

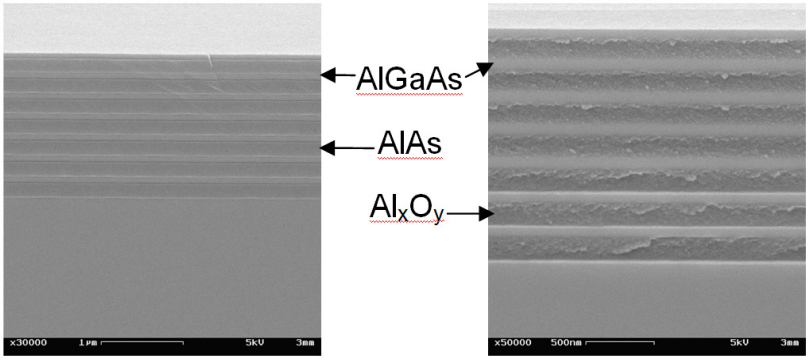

Figure 1) Scanning electron microscope images showing the as-grown oxidizable SBR with unoxidized AlAs layers (left) and the final SBR with fully oxidized Al_xO_y layers (right).

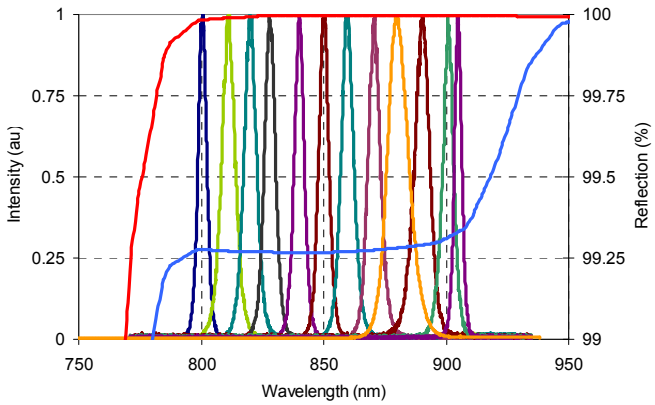

Figure 2) Example spectra from the Cr^{3+}:LiSAF laser, showing the tunability of the central wavelength of the laser from 800 nm to 905 nm, for the average ~140-fs pulses. The calculated small signal and saturated reflectivities of the SBR are also shown.

Publications

Journal Articles, Published

Duo Li, Umit Demirbas, Jonathan R. Birge, Gale S. Petrich, Leslie A. Kolodziejski, Alphan Sennaroglu, Franz X. Kärtner, and James G. Fujimoto, "Diode-pumped passively mode-locked GHz femtosecond Cr:LiSAF laser with kW peak power," Opt. Lett. 35, 1446-1448 (2010).

Umit Demirbas, Duo Li, Jonathan R. Birge, Alphan Sennaroglu, Gale S. Petrich, Leslie A. Kolodziejski, Franz X. Kaertner, and James G. Fujimoto, "Low-cost, single-mode diode-pumped Cr:Colquiriite lasers," Opt. Express 17, 14374-14388 (2009).

Meeting Papers, Published

E. Ippen, A. Benedick, J. Birge, H. Byun, L. -. Chen, G. Chang, D. Chao, J. Morse, A. Motamedi, M. Sander, G. Petrich, L. Kolodziejski, and F. Kärtner, "Optical Arbitrary Waveform Generation," in Quantum Electronics and Laser Science Conference, OSA Technical Digest (CD) (Optical Society of America, 2010), paper JThC4.

D. Li, U. Demirbas, J. R. Birge, G. S. Petrich, L. A. Kolodziejski, A. Sennaroglu, F. X. Kärtner, and J. G. Fujimoto, "Diode-Pumped Gigahertz Repetition Rate Femtosecond Cr:LiSAF Laser," in Conference on Lasers and Electro-Optics, OSA Technical Digest (CD) (Optical Society of America, 2010), paper CTuK3.

Umit Demirbas, Gale S. Petrich, Sheila Nabanja, Jonathan R.Birge, Leslie A.Kolodziejski, Franz X. Kartner, James G. Fujimoto, “Widely-tunable femtosecond operation of Cr:LiSAF lasers using broadband saturable Bragg reflectors” in Conference on Lasers and Electro-Optics (CLEO) and Quantum Electronics and Laser Science Conference (QELS), OSA Technical Digest (CD) (Optical Society of America, 2010), paper CThI3.

Michelle Y. Sander, Hyunil Byun, Jonathan Morse, David Chao, Hanfei M. Shen, Ali Motamedi, Gale Petrich, Leslie Kolodziejski, Erich P. Ippen, Franz X. Kartner, “1 GHz femtosecond erbium-doped fiber lasers” in Conference on Lasers and Electro-Optics (CLEO) and Quantum Electronics and Laser Science Conference (QELS), OSA Technical Digest (CD) (Optical Society of America, 2010), paper CTuII1.

A. Dergachev, P. F. Moulton, G. S. Petrich, L. A. Kolodziejski, and F. X. Kärtner, "Semiconductor Q-Switched, Short-Pulse, High-Power, MHz-Rate Laser," in Advanced Solid-State Photonics, OSA Technical Digest Series (CD) (Optical Society of America, 2010), paper AMC5.

James G Fujimoto, Franz X.Kartner, Alphan Sennaroglu, Leslie A. Kolodziejski, Gale S. Petrich, Peter Fendel, Hyunil Byun, Duo Li, Jonathan R. Birge, Kyung-Han Hong, Umit Demirbas, David A. Boas, Sava Sakadzic, “Recent advances in Cr: Colquiriite laser technology.” LEOS Annual Meeting Conference Proceedings, 2009. LEOS '09. IEEE. 2009. 387-388.

M. Araghchini, A. Yeng, M. Ghebrebrhan, I. Čelanović, J. Joannopoulos, G. S. Petrich, and L. A. Kolodziejski, "Optimization of Thermophotovoltaic Systems Using Tungsten Photonic Crystal Structures," in Optics and Photonics for Advanced Energy Technology, OSA Technical Digest (CD) (Optical Society of America, 2009), paper ThC7.